Journal of Thermal Analysis and Calorimetry, Vol. 61 (2000) 437–450

POLYPROPYLENE CRYSTALLIZATION IN AN ETHYLENE-PROPYLENE-DIENE RUBBER MATRIX

M. A. López Manchado[1], *J. Biagiotti*[2], *L. Torre*[2] *and J. M. Kenny*[2*]

[1]Institute of Polymer Science and Technology, Madrid, Spain
[2]Materials Engineering Center, University of Perugia, Loc. Pentima bassa 21, 05100 Terni, Italy

Abstract

The effect of the incorporation of an amorphous immiscible polymer (ethylene-propylene-diene-terpolymer) on the PP crystallization kinetics and thermodynamics is investigated by thermal analysis. The results of the investigation have shown that EPDM acts as a nucleant agent. A marked decrease of the half time of PP crystallization, $\tau_{1/2}$, as well as a sensible increase of the overall crystallization rate, K_n, has been observed in the presence of EPDM. Moreover, at any crystallization temperature, a minimum of $\tau_{1/2}$, is obtained at 25% EPDM content in the blend. The Avrami model has been successfully applied to describe the crystallization kinetics of the blend. The kinetic curves obtained under non-isothermal conditions confirm the results obtained under isothermal conditions and demonstrate the nucleant action of the EPDM phase on the PP crystallization.

Keywords: crystallization, EPDM, kinetics, morphology, PP, rubber

Introduction

Polyolefins, such as polypropylene (PP), are the thermoplastics of higher consumption because of their well-balanced physical and mechanical properties and their easy processability at a relatively low cost that makes them a versatile material. However, in some cases, not all the characteristics of this material are suitable for common service conditions. For instance, the relatively high PP glass transition temperature (T_g) renders it unsuitable for low-temperature applications. Thus, it is necessary to improve its flexibility and resilience at low temperatures [1, 2]. With this objective, impact modifiers have been added to PP and, among them, ethylene-propylene-diene-terpolymer (EPDM), due to its high impact strength over a wide range of temperature has been considered the most effective one [3–8]. These blends, commonly referred to as TPOs (polyolefin thermoplastic elastomers), are a special class of TPE that combines the processing characteristic of plastics at elevated temperatures [9–11] with the physical properties of conventional elastomers at service temperature [12, 13], playing an increasingly important role in the polymer material industry. Polyolefin

* Author to whom all correspondence should be addressed.

1418–2874/2000/ $ 5.00
Akadémiai Kiadó, Budapest

blends attract additional interest due to the possibility of recycling plastic wastes, avoiding the complex and expensive processes of separation of the different components. In a previous paper [14], the optimum conditions of processability have been determined and the mechanical properties-morphology correlation has also been examined. The results have shown the easy processability of PP-EPDM blends and a considerable improvement of their impact properties at low temperatures.

The study of the crystallization phenomena is of great importance in polymer processing. In particular, the study of the crystallization kinetics of polymers as a function of the processing conditions, from a macrokinetic point of view, is very important for the analysis and design of processing operations. On the other hand, physical properties of polymeric materials strongly depend on their microstructure and crystallinity, since it is at this microscopic level where failure of the materials takes place. To date, the most important aspects of polyolefin blends that have been investigated are reported to be influenced by their composition, morphology, mechanical behavior, melting temperature, crystallinity and crystallization rate during solidification from the melt. Calorimetry may be considered as one of the most interesting techniques for macrokinetic analysis of polymer crystallization. In particular, the crystallization kinetics of isotactic polypropylene (iPP) has been widely studied by different methods [15–19], and, in general, it has been well described by the Avrami equation [20, 21].

The PP-EPDM blend morphology has been recently discussed [22, 23] and the effects on the crystallization behavior of PP, in isothermal and non-isothermal experiments, have been investigated [24, 25]. The main goal of the present study is to apply thermal analysis to develop a kinetic model and to study the thermodynamic behavior of PP crystallization in the presence of an amorphous polymer (EPDM) on the whole range of rubber concentration.

Experimental

Materials

Commercially available grades of PP gently supplied by Montell and EPDM with 5-ethylidene–2-norborene (ENB) as a termonomer were used. The material specifications are listed in Table 1.

Melt-blended specimens of these homopolymers with various compositions were prepared in a Haake Rheomix 90 internal mixer equipped with a pair of high shear roller-type rotors. The temperature of the mixing chamber was set at 190°C and the blending time was 10 min. The rotor rate was set at 60 rpm. The obtained compounds were compression molded at 200°C in a Campana P3-34-E press during 15 min. Testing samples were cut from the molded plaques. Three different formulations were analyzed in this work. Pure PP and two different PP-EPDM blends: 75–25% and 50–50%. The crystallization conditions used in this study are reported in Table 2.

Table 1 Physical and mechanical characteristics of PP and EPDM

Material	iPP	EPDM
Manufacturer	Montell	Bayer
Designation	C 30 G	Buna EP T 6470P
Density/g cm^{-3}	0.92	0.86
Mooney viscosity ML (1+8) 125°C	–	55±5
Melt index/g 10 min^{-1}	6.0	–
Hardness/shore A	–	68.7

Table 2 Crystallization parameters of PP and PP-EPDM blends

Material PP–EPDM	T_c/°C	$\tau_{1/2}$/s	k/min^{-n}	n	T_m/°C	T_g/°C
	125	81	$3.25\cdot10^{-1}$	2.29	164.2	8.9
	127	126	$1.11\cdot10^{-1}$	2.40	164.8	
	130	275	$1.45\cdot10^{-2}$	2.54	165.9	
100–00	132	464	$3.97\cdot10^{-3}$	2.59	166.8	
	135	1013	$3.53\cdot10^{-4}$	2.58	169.0	
	137	1560	$1.86\cdot10^{-4}$	2.62	170.3	
	140	3120	$3.23\cdot10^{-5}$	2.65	171.5	
	125	60	$6.93\cdot10^{-1}$	2.18	164.9	8.1
	127	97	$1.99\cdot10^{-1}$	2.70	165.0	
	130	178	$4.14\cdot10^{-2}$	2.81	165.8	
75–25	132	275	$1.34\cdot10^{-2}$	2.69	166.8	
	135	627	$1.41\cdot10^{-3}$	2.64	167.6	
	137	958	$5.16\cdot10^{-4}$	2.60	170.0	
	140	1714	$1.17\cdot10^{-4}$	2.51	171.8	
	125	77	$3.64\cdot10^{-1}$	2.36	165.6	5.9
	127	131	$9.24\cdot10^{-2}$	2.70	166.1	
	130	213	$2.63\cdot10^{-2}$	2.61	166.4	
50–50	132	333	$8.30\cdot10^{-3}$	2.83	166.5	
	135	690	$1.27\cdot10^{-3}$	2.61	167.8	
	137	1200	$4.77\cdot10^{-4}$	2.43	169.1	
	140	2054	$7.62\cdot10^{-5}$	2.52	171.1	

Measurements

Isothermal and non-isothermal DSC tests were performed on the blends at different temperatures and cooling rates, respectively. Thermal analysis experiments were carried out in a DSC Perkin Elmer Pyris 1 differential scanning calorimeter coupled with

an intercooler. The following standard procedure was adopted. Samples of about 8 mg of mass were melted at 200°C for 10 min in order to eliminate any thermal history of the material; then they were cooled to the crystallization temperature, T_c and maintained to that temperature during the necessary time to complete the crystallization of the matrix. Seven crystallization temperatures have been examined in a range comprised between 125–140°C. The heat evolved during the isothermal crystallization (ΔH_c) was recorded as a function of time, at different crystallization temperatures. The experiments were carried out in nitrogen atmosphere and the scans after the crystallization isothermal tests were obtained at 10°C min^{-1}. Degree of crystallization curves were constructed by integrating the area under the exothermic peaks. On the other hand, the melting temperatures (T_m) of the blends were obtained from the maximum of the endothermic peaks.

The standard procedure performed in non-isothermal dynamic DSC scans was the following: samples of about 8 mg were heated from 30 to 200°C at a scan rate of 10°C min^{-1} and held for 10 min in order to eliminate any thermal history of the material. The samples were cooled to –50°C by using six prefixed scan rates in a range from 1 to 50°C min^{-1}. After crystallization the samples were heated to 200°C.

Results and discussion

Crystallization kinetics

The crystallization kinetics data of PP and PP-EPDM blends were interpreted on the basis of the Avrami analysis. The procedure requires the computation of the degree of crystallization (X_{mc}) obtained by integration of the area under the exothermic peak according to the following equation [26, 27]:

$$X_{mc}(t)=\frac{Q_{(t)}}{Q_f} \tag{1}$$

where $Q_{(t)}$ is the heat released during crystallization from the starting point to a generic time, obtained by partial integration of the curve, which is expressed in terms of the rate of heat evolution (dH/dt) as a function of time (t). Q_f is the heat of fusion of a perfect crystal taken as 209 J g^{-1} for polypropylene [28].

The application of the Avrami model requires the computation of the relative degree of crystallization given by:

$$X_r(t)=X_{mc}\frac{Q_f}{Q_\infty}=\frac{\int_0^t\left(\frac{dH}{dt}\right)dt}{\int_0^\infty\left(\frac{dH}{dt}\right)dt} \tag{2}$$

where Q_∞ is the total heat released during the crystallization process, obtained by total integration of the curve. Then, the Avrami model can now be used to describe the

development of the relative degree of crystallization in isothermal processes accordingly with the following equation:

$$X_r(t)=1-\exp(-kt^n) \quad (3)$$

where n is the Avrami exponent, k is the kinetic constant and t the crystallization time. These parameters, n and k, can be used to interpret qualitatively the nucleation mechanism, morphology and overall crystallization rate of the polymer. They can be calculated by plotting $\log(-\ln(1-X_r))$ *vs.* $\log(t)$ and evaluating the slope, which gives the Avrami exponent n, and the intercept, which gives the kinetic constant $\log k$. The value of k is also very often calculated from the equation [29]:

$$k=\frac{\ln 2}{(\tau_{1/2})^n} \quad (4)$$

where $\tau_{1/2}$ is the half time of crystallization, obtained at $X_r=0.5$.

Following the same approach, non-isothermal crystallization processes have been traditionally represented obtaining integral or differential expressions of the Avrami model with a temperature dependent kinetic constant. In particular, Nakamura *et al.* [30] proposed the following integral expression:

$$X_r(t)=1-\exp[-\int_0^t K(T)dt]^n \quad (5)$$

$K(T)$ is related to the Avrami constant in equation (3) through the relation:

$$K(T)=[k(T)^{1/n}] \quad (6)$$

Equation (5) reduces to the Avrami equation under isothermal conditions.

Isothermal crystallization

The results of the isothermal testing of PP crystallization are reported in Fig. 1 where DSC curves obtained by cooling the molten polymer to the isothermal crystallization temperature are shown. The slight delay in the DSC signal in the tests performed under isothermal conditions can not be simply attributed to an induction time effect due to nucleation. Nucleation is typically heterogeneous in most polymers used for commercial applications because the presence of catalyst residues and because nucleation agents are usually added in order to accelerate the overall crystallization process [30]. The apparent increase of induction time with the crystallization temperature may well be simply due to the slowing down of the overall crystallization rate (nucleation and growth) that reflects the instantaneous value of rate of heat release.

The strong effects of the temperature on the crystallization rate of PP are clearly observed in the isothermal DSC curves obtained on the neat polymer at different temperatures and reported in Fig. 1. These effects are still more evident from the degree of crystallization curves obtained by integration of Fig. 1 DSC curves and reported in Fig. 2. An increase of 10°C in the crystallization temperature involves an increase of more than 10 times the half time of crystallization.

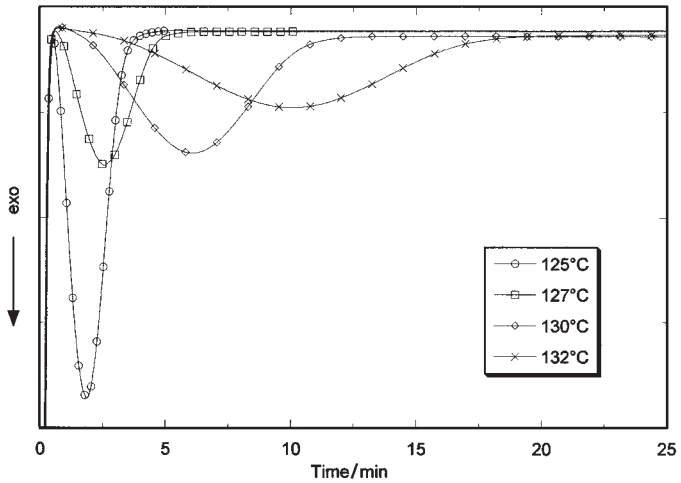

Fig. 1 Isothermal crystallization DSC curves of PP at different crystallization temperatures

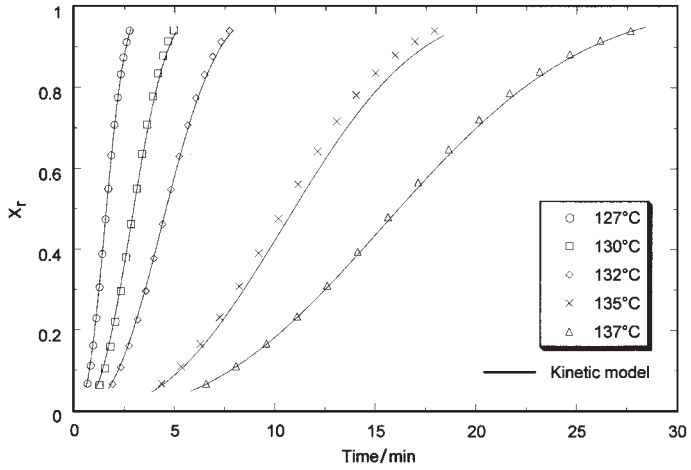

Fig. 2 Degree of crystallization of PP in isothermal processes at different temperatures

In the same manner, and to analyze the effects of the blend composition on PP crystallization, the crystallization isotherms and the degree of crystallization curves as a function of time of all the samples studied, obtained at 130°C, are represented in Figs 3 and 4, respectively. From these results, it can be deduced that the PP crystallization rate increases in presence of the EPDM and this increment is more evident at the lower concentration of the amorphous polymer (25%). Similar behavior was obtained at all the crystallization temperatures tested.

The effects of the rubber phase on the PP crystallization rate can be attributed to the modification of the PP matrix superstructure by the incorporation of the elastomer. Thus, a change of the average size and number of the spherulites is induced and this structural change is very important to interpret the function as impact modifier of the elastomer in the PP matrix. Moreover, the crystallization behavior of PP in the blend has also been attributed to the role of EPDM to selectively extract defective chains from the PP in the molten state [32]. This behavior should not be considered as a promotion of miscibility of both phases as demonstrated by the very slight changes of the measured T_g of the PP phase, obtained by DMA [33] and reported in Table 2.

However, at higher percentages of EPDM in the blend (50%) an inversion of the crystallization rate increase is observed. This behavior is clearly reflected analyzing the half time of crystallization as a function of the temperature (Fig. 5). From this fig-

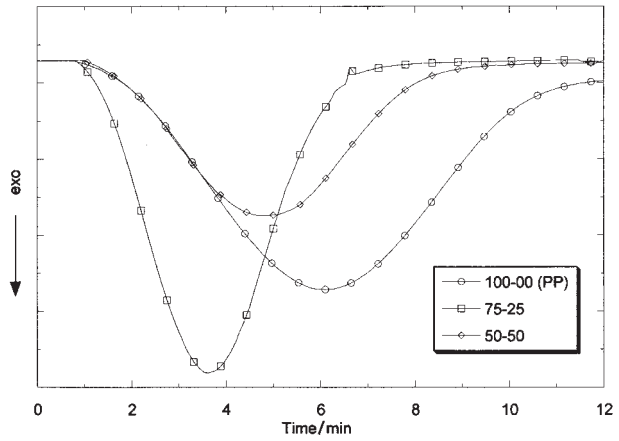

Fig. 3 Isothermal crystallization DSC curves of PP and PP-EPDM blends at 130°C

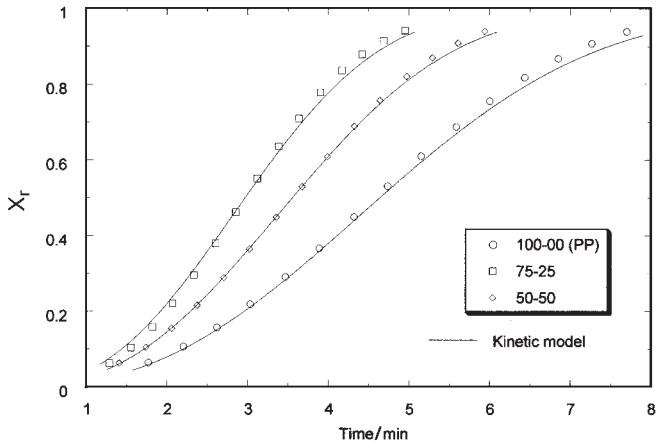

Fig. 4 Degree of crystallization of PP and PP-EPDM blends at 130°C

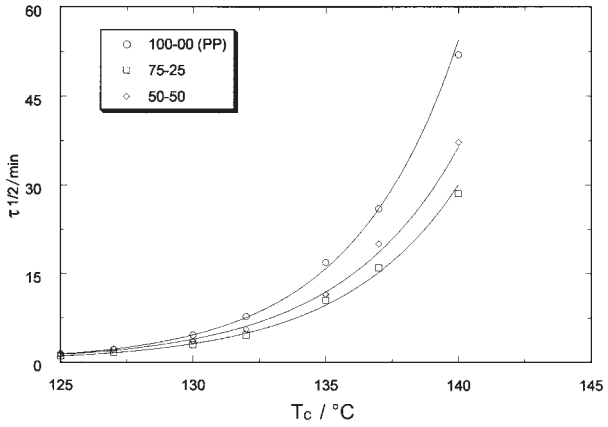

Fig. 5 Half time of PP crystallization ($\tau_{1/2}$) *vs.* crystallization temperature (T_c), in PP-EPDM blends. Continuous lines represent the model predictions

ure it can be deduced, in first place, that the half time increases with the crystallization temperature and, on the other hand, that the incorporation of the rubber increases the PP crystallization rate independently of the crystallization temperature. In addition, this increment is clearly higher for the blend with 25% of EPDM. The values of half times of PP crystallization ($\tau_{1/2}$) in the studied blends are reported in Table 2. As expected, when plotting the half time of PP crystallization *vs.* the EPDM content at different crystallization temperatures (Fig. 6), a minimum at 25% rubber content in the blend is observed.

The kinetic analysis was also performed by applying the Avrami model (Eq. (2)) in its logarithm form to the results of the isothermal crystallization processes of PP and of their blends. From these results, reported in Fig. 7, the Avrami parameters, n and the kinetic constants, k, of the different blends were calculated and are reported in Table 2. In all cases, fractional values of n were obtained and can be explained in terms of a partial overlapping of primary nucleation and crystal growth [34]. Following the evident parallelism of Avrami plots these values lie in a relatively narrow interval ($2<n<3$), and are traditionally attributed to a heterogeneous nucleation followed by diffusion controlled spherulitic crystalline growth.

The particular behavior observed on the crystallization kinetics of the blends could be explained through the balance of two opposite contributions. The results obtained suggest an increase of nucleation at the rubber-matrix interface with the rubber content while, on the other hand, the same rubber phase could be responsible of an impingement effect on the spherulitic growth. A similar behavior has been also reported in the study of the effects of carbon fibers on the crystallization behavior of different thermoplastic matrix composites [27, 35].

The values of the crystallization kinetic constant (k) (Table 2) have been normalized with the average value of n of the blends studied. These values confirm the in-

ferred conclusions from the analysis of $\tau_{1/2}$ values. That is, the crystallization rate of the polymer matrix decreases as the crystallization temperature increases and that EPDM acts as nucleating agent for the PP crystallization. At any crystallization temperature, the PP crystallization rate is higher in the presence of the amorphous polymer, showing a maximum for the PP-EPDM 75-25 blend.

The ability of the model to represent the crystallization behavior of the neat polymer and of the PP-EPDM blends is reported in Figs 2 and 4 where a very good agreement between experimental and theoretical curves for isothermal processes can be easily observed. Moreover, the model developed has been also used to predict the behavior of the crystallization half time as a function of the temperature in the isothermal processes. These predictions are well compared with the experimental values in Fig. 5.

The PP and PP-EPDM melting temperatures, determined as the maximum of the endothermic peaks obtained in DSC scans of the isothermally crystallized samples, are reported in Table 2. The melt temperature of the polypropylene increases as crystallization temperature increases (Fig. 8), which is directly related to the polymer crystallite size. However, T_m is not modified by the incorporation of EPDM in the blend.

Non-isothermal crystallization

The effects of EPDM on the crystallization of iPP have also been analyzed in non-isothermal DSC experiments. Figure 9 shows the dynamic DSC curves obtained on neat PP and PP-EPDM blends. The dynamic crystallization behavior observed confirms the results obtained in isothermal tests regarding the positive effects of the elastomeric phase on the crystallization kinetics of PP. The average values of the absolute degree of crystallinity (X_c), the crystallization peak (T_c) and the apparent melt-

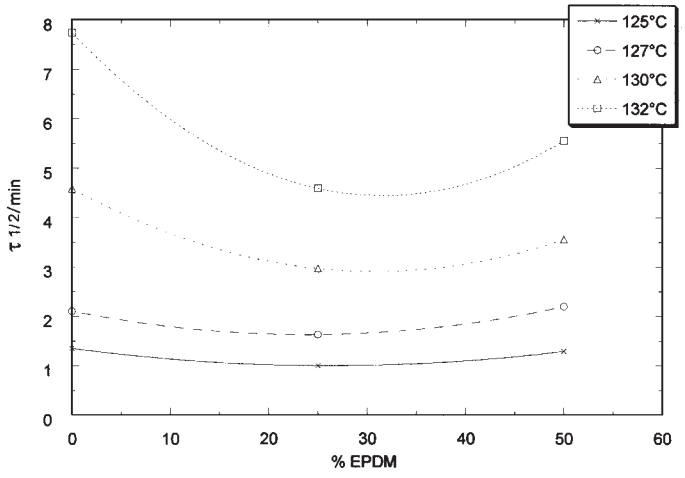

Fig. 6 Effect of EPDM content on the half time of PP crystallization ($\tau_{1/2}$)

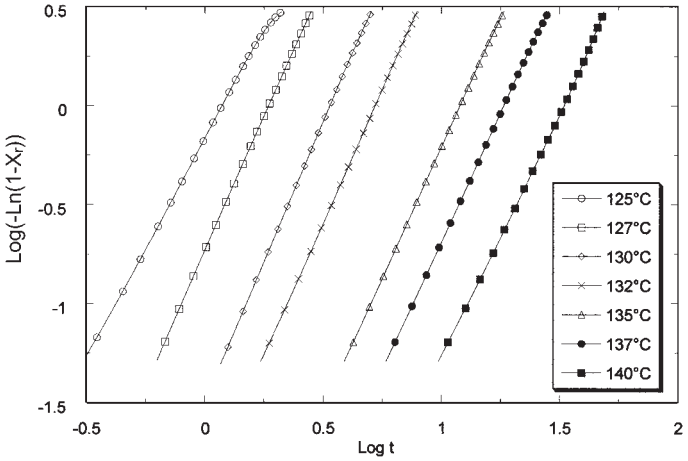

Fig. 7 Avrami plot of a 75-25 PP-EPDM blend at different temperatures

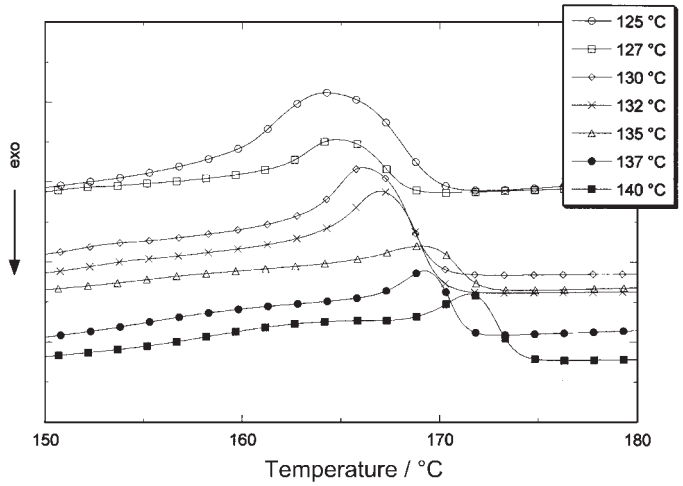

Fig. 8 DSC scans at 25°C min^{-1} of a 75-25 PP-EPDM blend showing the effect of the crystallization temperature

ing temperatures of the crystallized samples (T_m) are reported in Table 3. As in isothermal crystallization processes, T_c increases with the incorporation of the EPDM in the blend and this increment is more marked at lower rubber concentrations. This behavior is also evident when the results are expressed in terms of the relative degree of crystallization, computed by integration of the dynamic DSC curves, as reported in Fig. 10 for all the blends studied. These results confirm the nucleation ability of the EPDM on PP crystallization already detected in the isothermal analysis. It can be

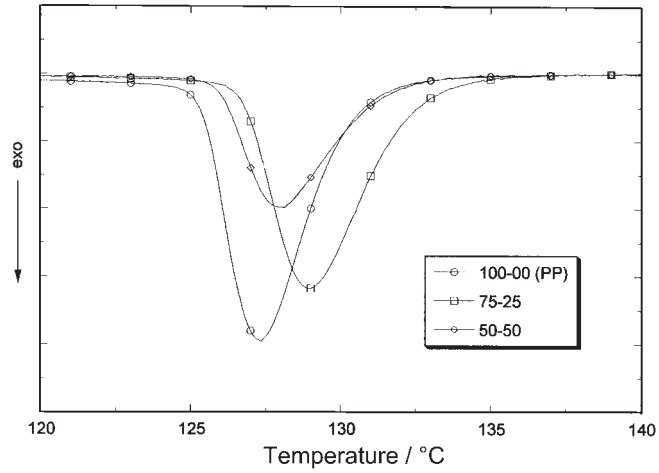

Fig. 9 Non-isothermal crystallization curves of PP and PP-EPDM blends at 1°C min^{-1}

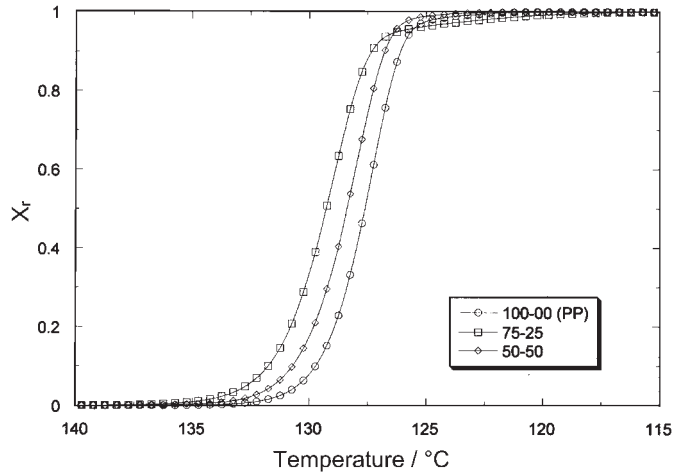

Fig. 10 Non-isothermal crystallization curves of PP and PP-EPDM blends at 1°C min^{-1}

concluded that the presence of the rubber produces more crystals leading to a faster overall crystallization behavior. However, no changes in the final absolute crystallinity fraction are detected. In fact, the decrease in the values of the crystallinity content observed in Table 3 with the addition of EPDM in the blend are directly associated to the dilution effects of the elastomer phase. Furthermore no changes in the melting point of the PP phase were detected in the blends.

Table 3 Melting temperature, crystallinity index and crystallinity peaks of PP and PP-EPDM blends

Material PP-EPDM	Cooling rate: 1°C min^{-1}			Cooling rate: 5°C min^{-1}			Cooling rate: 10°C min^{-1}		
	T_m/°C	X_r/%	T_c/°C	T_m/°C	X_r/%	T_c/°C	T_m/°C	X_r/%	T_c/°C
100–00	164.3	43	127.3	162.5	40	120.1	161.7	38	116.2
75–25	164.6	36	128.9	162.4	33	121.6	161.4	32	117.9
50–50	164.9	25	128.1	162.8	23	120.0	162.0	22	115.9
Material PP-EPDM	Cooling rate: 15°C min^{-1}			Cooling rate: 25°C min^{-1}			Cooling rate: 50°C min^{-1}		
	T_m/°C	X_r/%	T_c/°C	T_m/°C	X_r/%	T_c/°C	T_m/°C	X_r/%	T_c/°C
100–00	161.3	38	113.8	161.0	37	110.9	161.6	37	103.8
75–25	160.8	31	115.3	160.2	31	111.7	159.4	30	106.2
50–50	161.6	21	113.0	161.0	21	109.2	160.8	20	102.7

The dynamic crystallization analysis was also performed at different cooling rates. Dynamic results in terms of relative degree of crystallization as a function of temperature obtained on PP at three different cooling rates are reported in Fig. 11. Complete results on the neat PP and PP-EPDM blends are reported in Table 3. The shift in T_c with the cooling rate is directly associated to the thermal activation behavior of the crystallization process. The Nakamura model (Eq. (5)) with the same Avrami index obtained from isothermal results has been applied to the dynamic results. A reasonable agreement between experimental and theoretical curves for the non-isothermal crystallization processes on the blends studied is observed in Fig. 11.

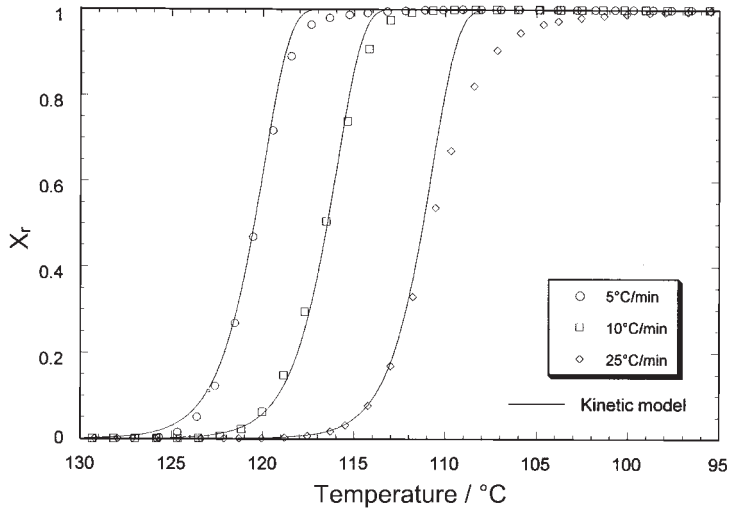

Fig. 11 Non-isothermal crystallization curves of PP at different cooling rates

Conclusions

Crystallization phenomena are of great importance in the study of the physical properties and the processing behavior of polymeric materials. It has been demonstrated how the incorporation of EPDM affects the crystalline behavior and structure of PP matrix and this change is very important to interpret the function of the elastomer as impact modifier within the PP matrix. It has been observed that EPDM rubber accelerates the nucleation and crystal growth mechanisms of PP, being this effect more appreciable at low rubber content (25%). This effect is attributed to the role of EPDM to selectively extract the defective molecules within PP and to offer a higher surface for crystal nucleation. On the other hand, the addition of EPDM does not affect the melting temperature of the PP matrix.

A good theoretical description of the crystallization behavior of PP in blends with EPDM has been obtained with the Avrami model which fractional values of n ($2<n<3$) confirm the heterogeneous nucleation of spherulitic crystals.

References

1 C. P. Rader, in Modern Plastic, R. Greene, Ed. New York 1992.
2 D. A. Thomas and L. K. Sperling in Polymers Blends, S. Newman and D.R. Paul, Eds. Academic Press, New York, Vol. 2, 1978.
3 A. N. Da Silva, M. B. Tavares, D. P. Politano, M. B. Coutinho and M. C. Rocha, J. Appl. Polym. Sci., 66 (1997) 2005.
4 B. M. Walker, Handbook of Thermoplastic Elastomers, Van Nostrand Reinhold, New York 1979.
5 A. Whelan and H. S. Lee, Development in Rubber Technology, J. Thermoplastic Rubbers, Applied Science, London 1982.
6 S. Thomas and A. George, Eur. Polym. J., 28 (1992) 1451.
7 D. S. Campbell, D. J. Elliot and M. A. Wheelans, N. R. Techno l, 9 (1978) 21.
8 Anon, Br. Plast. Rubber, 32 (1978).
9 D. J. Synrott, D. F. Sheidan and E. G. Kontos, in Thermoplastic Elastomers from Rubber-Plastic Blends, Ed. S. K. De and A. K. Bhowmick, Ellis Horwood, New York 1990.
10 N. M. Matthew and A. J. Tinker, J. Nat. Rubber. Res., 1 (1986) 240.
11 M. Batiuk, R. M. Harman and J. C. Healy, (to B. F. Goodrich Co.), US. Patent 3, 919, 358 (1975).
12 D. Hoppner and J. H. Wendorff, Colloid Polym. Sci., 268 (1990) 500.
13 J. Karger-Kocsis and I. Csiku, Polym. Eng. Sci., 27 (1987) 241.
14 M. A López Manchado, J. Biagiotti, M. Arroyo and J. Kenny, submitted to Polym. Eng. and Sci.
15 S. Hoshino, E. Meinecke, J. Power, R. Stein and S. Newman, J. Polym. Sci., Part 1, 3 (1995) 3041.
16 F. L. Bisbergen and B. DeLange, Polymer, 11 (1970) 309.
17 C. F. Pratt and S. Y. Hobbs, Polymer, 17 (1976) 12.
18 E. Martuscelli, M. Pracella, G. D. Volpe and P. Greco, Makromol. Chem., 185 (1984) 1041.
19 J. Jammak, S. Cheng, A. Zhang and E. Hsieh, Polymer, 33 (1992) 728.

20 M. J. Avrami, J. Chem. Phys., 7 (1939) 1103.
21 M. J. Avrami, J. Chem. Phys., 9 (1941) 177.
22 C. Y. Chen, Z.W. Yumus, H. Chin and T. Kyn, Polymer, (1997) 4433.
23 O. Chung and A. Y. Coran, Rubber Chemistry and Technology, 70 (1997) 781.
24 D. M. Bielinski, L. Slusarski, A. Wlochowicz, C. Slusarczyk and A. Pomllard, Polymer International, 44 (1997) 161.
25 Y. Yokoyama and T. Ricco, J. Appl. Polym. Sci., 66 (1997) 1007.
26 A. Maffezzoli, J. M. Kenny and L. Nicolais, Thermochim. Acta, 199 (1992) 133.
27 J. M. Kenny and A. Maffezzoli, Polym. Eng. Sci., 31 (1991) 607.
28 J. Brandrup and E. H. Immergut, Polymer Handbook, Vol. 24, Interscience Publishers, New York 1975.
29 B. Von Falkai, Makromol. Chem., 41 (1960) 86.
30 K. Nakamura, K. Katayama and T. Amano, J. Appl. Polym. Sci., 17 (1973) 1031.
31 B. Wunderlich, Macromolecular Physics, Academic Press, New York 1976.
32 E. Martuscelli, C. Silvestre and G. Abate, Polymer, 23 (1982) 229.
33 M. A. Lopez, J. Biagiotti and J. M. Kenny, sent to J. Appl. Polym. Sci.
34 L. Manderkern, Crystallization of Polymers. Mc Graw-Hill, New York 1964.
35 S. Saiello, J. M. Kenny and L. Nicolais, J. Materials Sci., 25 (1990) 3493.